



ORIGINAL ARTICLE

Advances in numerical simulation with a clustering method based on K-means algorithm and Adams Bashforth scheme for fractional order laser chaotic system



Muhammad Sinan^a, Jinsong Leng^a, Kamal Shah^{b,c}, Thabet Abdeljawad^{b,d,e,*}

^a School of Mathematical Sciences, University of Electronic Science and Technology of China, Chengdu 611731, China

^b Department of Mathematics and Sciences, Prince Sultan University, P.O. Box 66833, 11586 Riyadh, Saudi Arabia

^c Department of Mathematics, University of Malakand, Dir(L), Khyber Pakhtunkhwa, Pakistan

^d Department of Medical Research, China Medical University, Taichung 40402, Taiwan

^e Department of Mathematics Kyung Hee University, 26 Kyungheedaero-ro, Dongdaemungu, Seoul 02447, Republic of Korea

Received 18 May 2022; revised 26 April 2023; accepted 21 May 2023

Available online 1 June 2023

KEYWORDS

Qualitative theory;
Chaotic behavior;
K-Means algorithm;
A clustering method;
Adams Bashforth Scheme

MATHEMATICS
SUBJECT
CLASSIFICATION

37D45;
37M99;
37M05;
93A30

Abstract In this research work, we present a mathematical analysis of a fractional sixth-order laser model of a resonant which is homogeneously extended three-level optically pumped. We use Caputo fractional order derivative in the proposed model. Our analysis includes an investigation of various chaotic behaviors under fractional order derivative and qualitative theory of the existence of the solution to the proposed model. For our required analysis of qualitative type, we use formal analysis tools. Further, numerical simulations are performed with a clustering method based on the K-Means algorithm and Adams Bashforth scheme. With the help of the aforesaid scheme, we present different chaotic behavior corresponding to various values of fractional order. Finally, we give a comparison of the CPU time of the proposed method with that of the RK4 method.

© 2023 THE AUTHORS. Published by Elsevier BV on behalf of Faculty of Engineering, Alexandria University. This is an open access article under the CC BY-NC-ND license (<http://creativecommons.org/licenses/by-nc-nd/4.0/>).

1. Introduction

In the previous few years, the area devoted to investigating various non-linear dynamic behaviors of optically pumped, far infrared laser models has been given much attention. For a deep understanding of the homoclinic theory of bifurcation with the help of some specific applications of nonlinear optics to demonstrate the universality of the causes and the rules subject to deterministic chaotic dynamics has been presented. For

* Corresponding author at: Department of Mathematics and Sciences, Prince Sultan University, P.O. Box 66833, 11586 Riyadh, Saudi Arabia. Department of Medical Research, China Medical University, Taichung 40402, Taiwan.

E-mail addresses: sinanmathematics@gmail.com, 202124110102@std.uestc.edu.cn (M. Sinan), tabdeljawad@psu.edu.sa (T. Abdeljawad).

Peer review under responsibility of Faculty of Engineering, Alexandria University.

instance, authors, [1] have studied regular and chaotic dynamics of optically pumped molecular lasers. In the same line, a detailed bifurcations analysis for an optically pumped three-level laser model has been given in [2]. Also, homoclinic puzzles and chaos in a nonlinear laser model have been investigated in [4]. Further, some specific observations and many experiments performed in past have been compared with the two-level Haken-Lorenz laser mode in [5]. The OPL model under classical differential equations have been discussed in [1–3]. The concerned model is given by

$$\begin{aligned}
 \frac{df_1}{dt} &= -\alpha_1 f_1 + \alpha_2 f_3, \\
 \frac{df_2}{dt} &= -f_2 - f_1 f_4 + \alpha_3 g_1, \\
 \frac{df_3}{dt} &= -f_3 + f_1 g_2 - \alpha_3 f_4, \\
 \frac{df_4}{dt} &= -f_4 + f_1 f_2 + \alpha_3 f_3, \\
 \frac{dg_1}{dt} &= -\alpha_4 (g_1 - g_1^0) - 4\alpha_3 f_2 - 2f_1 f_3, \\
 \frac{dg_2}{dt} &= -\alpha_4 (g_2 - g_2^0) - 2\alpha_3 f_2 - 4f_1 f_3.
 \end{aligned} \tag{1}$$

Where, classes are defined as: f_1 Rabi flopping quantity representing the electric field amplitude at emission frequency, f_2, f_3 , and f_4 are the normalized density matrix elements, g_1 and g_2 are the population differences. α_1 represents the cavity loss parameter, α_2 is the unsaturated gain, α_3 Rabi flopping quantity represents the electric field amplitudes at pump frequency, and α_4 is the ratio between population and polarization. So far, we know the ordinary derivative has been exercised very well for the aforementioned area.

Here we remark that fractional calculus is a powerful tool to investigate various dynamical problems for detailed analysis and information. Because fractional order derivative of a function gives the accumulation results which include the integer order counterpart as a special case. Further, with the help of fractional order derivatives, we can understand the complex geometry of various phenomena and processes of the real-world more properly. The mentioned area has been used very well in applied problems. For instance authors, [6] have studied the dynamics of the fractal-fractional model of a new chaotic system of an integrated circuit with a Mittag–Leffler kernel. In the same way, author [7] has given a detailed analysis of fractional order derivatives and integrals. Author [8] has established various results for fractional order derivatives and integrals. Authors [9] have established numerical methods for fractional differentiation. The concepts of fractional calculus have been very used in mathematical modeling of biology and other fields of sciences in [10,25–27].

Keeping in mind the importance of fractional calculus, in this paper, we extend the laser model (1) to fractional order under the Caputo derivative as:

$$\begin{aligned}
 {}_0^c \mathcal{D}_t^\kappa f_1(t) &= -\alpha_1 f_1 + \alpha_2 f_3, \\
 {}_0^c \mathcal{D}_t^\kappa f_2(t) &= -f_2 - f_1 f_4 + \alpha_3 g_1, \\
 {}_0^c \mathcal{D}_t^\kappa f_3(t) &= -f_3 + f_1 g_2 - \alpha_3 f_4, \\
 {}_0^c \mathcal{D}_t^\kappa f_4(t) &= -f_4 + f_1 f_2 + \alpha_3 f_3, \\
 {}_0^c \mathcal{D}_t^\kappa g_1(t) &= -\alpha_4 (g_1 - g_1^0) - 4\alpha_3 f_2 - 2f_1 f_3, \\
 {}_0^c \mathcal{D}_t^\kappa g_2(t) &= -\alpha_4 (g_2 - g_2^0) - 2\alpha_3 f_2 - 4f_1 f_3.
 \end{aligned} \tag{2}$$

We develop a Cluster-based method as already has been used for reduced-order modeling of a mixing layer in [12] to treat the considered model. Our proposed scheme is based on the K-Mean type algorithm [13] and Adam-Bashforth numerical scheme. We construct the numerical algorithm by using the

aforsaid methods for our proposed model under the fractional order derivative. We simulate the results under various values of parameters and fractional order to detect different chaotic dynamical behaviors of different compartments of the model.

Here we remark that Cluster analysis itself is not one explicit procedure, but it is used to solve many general tasks. For the mentioned purposes, various algorithms have been used. The further cluster has no unique definition. Therefore, numerous algorithms have been designed for it. Hence clustering algorithms can be categorized based on their cluster model. Here some famous various types of clustering algorithms that have been increasingly used to handle all kinds of unique data are Density-based, Centroid-based, Hierarchical-based, K-means clustering algorithm, etc. Among the said cluster algorithms, K-Mean is a powerful method. In the mentioned method, each cluster is described by a central vector, which is not necessarily a member of the data set. The K-Means clustering algorithm has some advantages like being simple to implement, guaranteeing convergence, scaling to large data sets, easy for selecting new examples, etc. However, there are some disadvantages also exist, for instance, depending on initial data. Further on increasing the number of dimensions, the convergence of the method suffered. For the detailed merits and de-merits see [14].

Also, we established some qualitative results for the existence and uniqueness of the solution to the model under consideration. For this purpose, we apply the Banach theorem and some tools of nonlinear analysis. Here it should be kept in mind that chaos is a periodic long-term behavior in a deterministic system that exhibits sensitive dependence on initial conditions. We will investigate the said behavior under the fractional order derivative for our model. Here we inform the readers that chaotic behaviors of various dynamical systems for fractional order derivatives have been studied in the last few years very well. For instance authors, [15] have described modeling attractors of chaotic dynamical systems with fractal-fractional operators. In the same way, the chaotic behavior of the Bloch model with a delay has been studied in [16]. Also, chaos synchronization of fractional chaotic maps based on the stability condition has been investigated in [17,18]. Further authors [19] have studied a generating chaotic system with one stable equilibrium.

The structure of the manuscript is arranged in the following form: in first Section 1 we introduce the goal of the manuscript and the applications of the proposed algorithm Subsection 1.1 along with some preliminary results Subsection 1.2. In Section 3, the existence and uniqueness of solution the model (2) is presented. In Section 4, for the solution of the model (2) the numerical scheme is presented. In Section 5, the K-Means Clustering Algorithm is presented. In Section 6, the graphical results of the manuscript are discussed. While the whole manuscript is concluded in Section 7.

1.1. Applications of K-means Algorithm

In real life, K-Means clustering is employed in a range of situations, including diagnostic systems where the medical industry employs it to develop smarter medical decision support systems, particularly in the treatment of liver disorders. Clustering is a fundamental component of search engines. The

search engines frequently utilize clustering to organize the search results once a search has been conducted. In contrast, the clustering algorithm in wireless sensor networks is responsible for identifying the cluster heads that gather all the data for each cluster. To read about other applications, one can read [20–24,28,29].

1.2. Preliminaries

Here, we describe some fundamental results which are using onward in further analysis.

Definition 1.1. Suppose, we consider the generic piecewise fractional order differential equation with fractional order κ , such that

$${}^c \mathcal{D}_t^\kappa u(t) = \rho(t, u(t)), \text{ with } u(0) = u_0. \tag{3}$$

For the differential Eq. (3) we define Fractional Adams–Bashforth Scheme [10] with Caputo Derivative that is:

$$\begin{aligned} \mathfrak{I}(t_{q+1}) = & \mathfrak{I}(t_q) + \frac{\varphi(t_q, \mathfrak{I}_q)}{h\Gamma(\kappa)} \left\{ \frac{2h}{\kappa} t_{q+1}^\kappa - \frac{t_{q+1}^{\kappa+1}}{\kappa+1} + \frac{h}{\kappa} t_q^\kappa - \frac{t_q^{\kappa+1}}{\kappa} \right\} \\ & + \frac{\varphi(t_{q-1}, \mathfrak{I}_{q-1})}{h\Gamma(\kappa)} \left\{ \frac{h}{\kappa} t_{q+1}^\kappa - \frac{t_{q+1}^{\kappa+1}}{\kappa+1} + \frac{t_q^\kappa}{\kappa+1} \right\}. \end{aligned} \tag{4}$$

Definition 1.2. Suppose that, X and Z are two samples of pattern vectors,

$V = (v_1, v_2, v_3, \dots, v_n)^T$ $U = (u_1, u_2, u_3, \dots, u_n)^T$ and we define the distance between V and U as:

$$D = \|V - U\| = \left[\sum_{j=1}^n (v_j - u_j)^2 \right]^{\frac{1}{2}}.$$

Easy to know that the smaller D is, the more similar are V and U (D is the Norm [10] of V and U in n dimensional space)

Definition 1.3.

With a cone, suppose we have a real Banach Space \mathbb{B} and in restricted order namely φ in Banach Space in supersede approach such that $v \leq u$. That implies that $u - v \in \varphi$, while $v \leq w$ such that $w - v \in \varphi, \forall v, u, w \in \mathbb{B}$. Furthermore, we have $\langle \bar{a}, \bar{b} \rangle = \{f \in \mathcal{B} : \bar{a} \leq f \leq \bar{b}\}$ is the order of interval. If there is a feasibility of obtaining a constant $a_1 > 0$, then cone φ is denoted as normal that is $a_2, a_3 \in \varphi, \phi < a_2 < a_3 \Rightarrow \|a_2\| \leq \|a_3\|$, where the zeros of φ is ϕ .

2. Dissipation of the proposed model

The considered model given in system (1) is dissipative as earlier been discussed in [6] as

$$\begin{aligned} \nabla V = & \frac{\partial}{\partial f_1} \left(\frac{df_1}{dt} \right) + \frac{\partial}{\partial f_2} \left(\frac{df_2}{dt} \right) + \frac{\partial}{\partial f_3} \left(\frac{df_3}{dt} \right) + \frac{\partial}{\partial f_4} \left(\frac{df_4}{dt} \right) \\ & + \frac{\partial}{\partial g_1} \left(\frac{dg_1}{dt} \right) + \frac{\partial}{\partial g_2} \left(\frac{dg_2}{dt} \right), \end{aligned} \tag{5}$$

such that for positive values of parameters, we have

$$-(3 + 2\alpha_4 + 2\alpha_3 + \alpha_1) < 0. \tag{6}$$

3. Existence and uniqueness

Suppose, in all smooth real function bounded in a closed set $[\bar{a}, \bar{b}]$ we define the Banach space B such that $\mathbb{B} = \mathbb{C}_{\bar{a}, \bar{b}}$ containing a sub-norm. While, the given shaft such as $\bar{S} = \{v_1, v_2, v_3 \in \bar{S}, v_1(y, t) \geq 0, v_2(y, t) \geq 0, \text{ and } v_3(y, t) \geq 0, \bar{a} \leq t \leq \bar{b}\}$. We study the following fractional system (2) with Caputo operator and apply the fundamental theorem of calculus to check the existence of solution.

$$\left. \begin{aligned} f_1(t) - f_1(0) &= \frac{1}{\Gamma(\kappa)} \int_0^t (-\alpha_1 f_1 + \alpha_2 f_3)(t - \tau)^{\kappa-1} d\tau, \\ f_2(t) - f_2(0) &= \frac{1}{\Gamma(\kappa)} \int_0^t (-f_2 - f_1 f_4 + \alpha_3 g_1)(t - \tau)^{\kappa-1} d\tau, \\ f_3(t) - f_3(0) &= \frac{1}{\Gamma(\kappa)} \int_0^t (-f_3 + f_1 g_2 - \alpha_3 f_4)(t - \tau)^{\kappa-1} d\tau, \\ f_4(t) - f_4(0) &= \frac{1}{\Gamma(\kappa)} \int_0^t (-f_4 + f_1 f_2 + \alpha_3 f_3)(t - \tau)^{\kappa-1} d\tau, \\ g_1(t) - g_1(0) &= \frac{1}{\Gamma(\kappa)} \int_0^t (-\alpha_4 (g_1 - g_1^0) - 4\alpha_3 f_2 - 2f_1 f_3)(t - \tau)^{\kappa-1} d\tau, \\ g_2(t) - g_2(0) &= \frac{1}{\Gamma(\kappa)} \int_0^t (-\alpha_4 (g_2 - g_2^0) - 2\alpha_3 f_2 - 4f_1 f_3)(t - \tau)^{\kappa-1} d\tau. \end{aligned} \right\} \tag{7}$$

Next, we have a compact $\mathbb{C}_{\bar{a}, \bar{b}}$ given below, that is

$$\mathbb{C}_{\bar{a}, \bar{b}} = I_{\bar{a}}(t_0) \times \mathbb{B}_{\bar{b}}(\xi), \tag{8}$$

where

$$\xi = \min \{f_{10}, f_{20}, f_{30}, f_{40}, g_{10}, g_{20}\}, \tag{9}$$

also

$$I_{\bar{a}}(t_0) = [t_0 - \bar{a}, t_0 + \bar{a}], \quad \mathbb{B}_0(\xi) = [\xi - \bar{b}, \xi + \bar{b}]. \tag{10}$$

Suppose

$$\left. \begin{aligned} z_1(f_1, f_2, f_3, f_4, g_1, g_2, t) &= -\alpha_1 f_1 + \alpha_2 f_3, \\ z_2(f_1, f_2, f_3, f_4, g_1, g_2, t) &= -f_2 - f_1 f_4 + \alpha_3 g_1, \\ z_3(f_1, f_2, f_3, f_4, g_1, g_2, t) &= -f_3 + f_1 g_2 - \alpha_3 f_4, \\ z_4(f_1, f_2, f_3, f_4, g_1, g_2, t) &= -f_4 + f_1 f_2 + \alpha_3 f_3, \\ z_5(f_1, f_2, f_3, f_4, g_1, g_2, t) &= -\alpha_4 (g_1 - g_1^0) - 4\alpha_3 f_2 - 2f_1 f_3, \\ z_6(f_1, f_2, f_3, f_4, g_1, g_2, t) &= -\alpha_4 (g_2 - g_2^0) - 2\alpha_3 f_2 - 4f_1 f_3. \end{aligned} \right\} \tag{11}$$

Also, we assume

$$\mathbb{Q} = \max \left\{ \sup_{\mathbb{C}_{\bar{a}, \bar{b}}} \|z_1\|, \sup_{\mathbb{C}_{\bar{a}, \bar{b}}} \|z_2\|, \sup_{\mathbb{C}_{\bar{a}, \bar{b}}} \|z_3\|, \sup_{\mathbb{C}_{\bar{a}, \bar{b}}} \|z_4\|, \sup_{\mathbb{C}_{\bar{a}, \bar{b}}} \|z_5\|, \sup_{\mathbb{C}_{\bar{a}, \bar{b}}} \|z_6\| \right\}. \tag{12}$$

We have adopted the infinite norm by doing so,

$$\|\varphi\|_\infty = \sup_{t \in I_{\bar{a}}} \|\varphi(t)\|. \tag{13}$$

Furthermore, we build a mapping, namely

$$\Lambda : \mathbb{C}_{\bar{a}, \bar{b}} \rightarrow \mathbb{C}_{\bar{a}, \bar{b}}, \tag{14}$$

so that

$$\Lambda F(t) = F_0 + \frac{1}{\Gamma(\kappa)} \int_0^t G(f_1, f_2, f_3, f_4, g_1, g_2, t)(t - \tau)^{\kappa-1} d\tau, \tag{15}$$

with

$$F(t) = \begin{pmatrix} f_1(t) \\ f_2(t) \\ f_3(t) \\ f_4(t) \\ g_1(t) \\ g_2(t) \end{pmatrix}, \tag{16}$$

$$G(f_1, f_2, f_3, f_4, g_1, g_2, t) = \begin{pmatrix} z_1(f_1, f_2, f_3, f_4, g_1, g_2, t) \\ z_2(f_1, f_2, f_3, f_4, g_1, g_2, t) \\ z_3(f_1, f_2, f_3, f_4, g_1, g_2, t) \\ z_4(f_1, f_2, f_3, f_4, g_1, g_2, t) \\ z_5(f_1, f_2, f_3, f_4, g_1, g_2, t) \\ z_6(f_1, f_2, f_3, f_4, g_1, g_2, t) \end{pmatrix}.$$

We must show that the new fractional operator is well defined, that is, we evaluate the condition for which

$$\|\Lambda F(t) - F_0\|_\infty < \begin{pmatrix} \bar{b} \\ \bar{b} \\ \bar{b} \\ \bar{b} \\ \bar{b} \\ \bar{b} \end{pmatrix}, \quad \text{where} \quad \left\{ \begin{array}{l} \|\Lambda_1 f_1(t) - f_{10}\|_\infty < \bar{b}, \\ \|\Lambda_2 f_2(t) - f_{20}\|_\infty < \bar{b}, \\ \|\Lambda_3 f_3(t) - f_{30}\|_\infty < \bar{b}, \\ \|\Lambda_4 f_4(t) - f_{40}\|_\infty < \bar{b}, \\ \|\Lambda_2 f_5(t) - f_{50}\|_\infty < \bar{b}, \\ \|\Lambda_3 f_6(t) - f_{60}\|_\infty < \bar{b}. \end{array} \right. \tag{17}$$

We'll begin with the z_1 component, that is:

$$\begin{aligned} \|\Lambda_1 f_1(t) - f_{10}\|_\infty &= \left\| \frac{1}{\Gamma(\kappa)} \int_0^t z_1(f_1, f_2, f_3, f_4, g_1, g_2, \tau)(t - \tau)^{\kappa-1} d\tau \right\|_\infty, \\ &\leq \frac{1}{\Gamma(\kappa)} \int_0^t \|z_1(f_1, f_2, f_3, f_4, g_1, g_2, \tau)\|_\infty (t - \tau)^{\kappa-1} d\tau, \\ &\leq \frac{Q}{\Gamma(\kappa)} \int_0^t (t - \tau)^{\kappa-1} d\tau, \\ &\leq \frac{Q\bar{a}^\kappa}{\Gamma(\kappa+1)} < \bar{b}, \end{aligned} \tag{18}$$

where

$$\bar{a} < \left(\frac{\bar{b}\Gamma(\kappa+1)}{Q} \right)^{1/\kappa}. \tag{19}$$

Similarly, for the remaining components, we have

$$\begin{aligned} \|\Lambda_2 f_2(t) - f_{20}\|_\infty &< \frac{Q\bar{a}^\kappa}{\Gamma(\kappa+1)}, \\ \|\Lambda_2 f_3(t) - f_{30}\|_\infty &< \frac{Q\bar{a}^\kappa}{\Gamma(\kappa+1)}, \\ \|\Lambda_2 f_4(t) - f_{40}\|_\infty &< \frac{Q\bar{a}^\kappa}{\Gamma(\kappa+1)}, \\ \|\Lambda_2 g_1(t) - g_{10}\|_\infty &< \frac{Q\bar{a}^\kappa}{\Gamma(\kappa+1)}, \end{aligned} \tag{20}$$

and

$$\|\Lambda_2 g_2(t) - g_{20}\|_\infty < \frac{Q\bar{a}^\kappa}{\Gamma(\kappa+1)}. \tag{21}$$

Thus

$$\|\Gamma F(t) - F_0\|_\infty \leq \frac{Q\bar{a}^\kappa}{\Gamma(\kappa+1)}. \tag{22}$$

Γ is well defined if $\bar{a} < \left(\frac{\bar{b}\Gamma(\kappa+1)}{Q} \right)^{1/\kappa}$. Second, we require to show that our function has a Lipshitz condition. That is

$$\|\Gamma F_1 - \Gamma F_2\|_\infty < K\|F_1 - F_2\|. \tag{23}$$

Implies that:

$$\begin{aligned} \|\Lambda_1 f_{11} - \Lambda_1 f_{12}\|_\infty &= \left\| \frac{1}{\Gamma(\kappa)} \int_0^t z_1(f_{11}, f_{21}, f_{31}, f_{41}, g_1, g_2, \tau)(t - \tau)^{\kappa-1} d\tau \right. \\ &\quad \left. - \frac{1}{\Gamma(\kappa)} \int_0^t z_1(f_{12}, f_{22}, f_{32}, f_{42}, g_1, g_2, \tau)(t - \tau)^{\kappa-1} d\tau \right\|_\infty, \\ &\leq \frac{1}{\Gamma(\kappa)} \int_0^t \|z_1(f_{11}, f_{21}, f_{31}, f_{41}, g_1, g_2, \tau) - z_1(f_{12}, f_{22}, f_{32}, f_{42}, g_1, \\ &\quad g_2, \tau)\|_\infty (t - \tau)^{\kappa-1} d\tau, \\ &\leq \frac{1}{\Gamma(\kappa)} \int_0^t \|\alpha_1 f_{11} + \alpha_2 f_{31} + \alpha_1 f_{12} - \alpha_2 f_{32}\|_\infty (t - \tau)^{\kappa-1} d\tau, \\ &\leq \frac{|\alpha_1|}{\Gamma(\kappa)} \int_0^t \|f_{12} - f_{11}\|_\infty (t - \tau)^{\kappa-1} d\tau < \frac{|\alpha_1|}{\Gamma(\kappa)} \|f_{12} - f_{11}\|_\infty \cdot \frac{\bar{a}^\kappa}{\kappa}, \\ &\leq \frac{|\alpha_1| \|f_{12} - f_{11}\|_\infty \bar{a}^\kappa}{\Gamma(\kappa+1)} \leq \|f_{12} - f_{11}\|_\infty \Lambda_1, \end{aligned} \tag{24}$$

where

$$\gamma_1 = \frac{|\alpha_1| \bar{a}^\kappa}{\Gamma(\kappa+1)}. \tag{25}$$

For the second component:

$$\begin{aligned} \|\Lambda_2 f_{21} - \Lambda_2 f_{22}\|_\infty &= \left\| \frac{1}{\Gamma(\kappa)} \int_0^t z_2(f_{11}, f_{21}, f_{31}, f_{41}, g_1, g_2, \tau)(t - \tau)^{\kappa-1} d\tau \right. \\ &\quad \left. - \frac{1}{\Gamma(\kappa)} \int_0^t z_2(f_{12}, f_{22}, f_{32}, f_{42}, g_1, g_2, \tau)(t - \tau)^{\kappa-1} d\tau \right\|_\infty, \\ &\leq \frac{1}{\Gamma(\kappa)} \int_0^t \|z_2(f_{11}, f_{21}, f_{31}, f_{41}, g_1, g_2, \tau) - z_2(f_{12}, f_{22}, f_{32}, f_{42}, g_1, \\ &\quad g_2, \tau)\|_\infty (t - \tau)^{\kappa-1} d\tau, \\ &\leq \frac{1}{\Gamma(\kappa)} \int_0^t \|-f_{21} - f_{12} + \alpha_3 g_1 + f_{22} + f_{11} - \alpha_3 g_1\|_\infty (t - \tau)^{\kappa-1} d\tau, \\ &\leq \frac{1}{\Gamma(\kappa)} \int_0^t \|f_{22} - f_{21}\|_\infty (t - \tau)^{\kappa-1} d\tau < \frac{1}{\Gamma(\kappa)} \|f_{22} - f_{21}\|_\infty \cdot \frac{\bar{a}^\kappa}{\kappa}, \\ &\leq \frac{\|f_{22} - f_{21}\|_\infty \bar{a}^\kappa}{\Gamma(\kappa+1)} \leq \|f_{22} - f_{21}\|_\infty \gamma_2, \end{aligned} \tag{26}$$

where

$$\gamma_2 = \frac{\bar{a}^\kappa}{\Gamma(\kappa+1)}. \tag{27}$$

For the third component:

$$\begin{aligned} \|\Lambda_3 f_{31} - \Lambda_3 f_{32}\|_\infty &= \left\| \frac{1}{\Gamma(\kappa)} \int_0^t z_3(f_{11}, f_{21}, f_{31}, f_{41}, g_1, g_2, \tau)(t - \tau)^{\kappa-1} d\tau \right. \\ &\quad \left. - \frac{1}{\Gamma(\kappa)} \int_0^t z_3(f_{12}, f_{22}, f_{32}, f_{42}, g_1, g_2, \tau)(t - \tau)^{\kappa-1} d\tau \right\|_\infty, \\ &\leq \frac{1}{\Gamma(\kappa)} \int_0^t \|z_3(f_{11}, f_{21}, f_{31}, f_{41}, g_1, g_2, \tau) - z_3(f_{12}, f_{22}, f_{32}, f_{42}, g_1, g_2, \tau)\|_\infty (t - \tau)^{\kappa-1} d\tau, \\ &\leq \frac{1}{\Gamma(\kappa)} \int_0^t \|-f_{31} + f_{12} - \alpha_3 f_4 + f_{32} - f_{11} + \alpha_3 f_4\|_\infty (t - \tau)^{\kappa-1} d\tau, \\ &\leq \frac{1}{\Gamma(\kappa)} \int_0^t \|f_{32} - f_{31}\|_\infty (t - \tau)^{\kappa-1} d\tau < \frac{1}{\Gamma(\kappa)} \|f_{32} - f_{31}\|_\infty \cdot \frac{\bar{a}^\kappa}{\kappa}, \\ &\leq \frac{\|f_{32} - f_{31}\|_\infty \bar{a}^\kappa}{\Gamma(\kappa+1)} \leq \|f_{32} - f_{31}\|_\infty \gamma_3, \end{aligned} \tag{28}$$

where

$$\gamma_3 = \frac{\bar{a}^\kappa}{\Gamma(\kappa+1)}. \tag{29}$$

For fourth component:

$$\begin{aligned} \|\Lambda_4 f_{41} - \Lambda_4 f_{42}\|_\infty &= \left\| \frac{1}{\Gamma(\kappa)} \int_0^t z_4(f_{11}, f_{21}, f_{31}, f_{41}, g_1, g_2, \tau)(t - \tau)^{\kappa-1} d\tau \right. \\ &\quad \left. - \frac{1}{\Gamma(\kappa)} \int_0^t z_4(f_{12}, f_{22}, f_{32}, f_{42}, g_1, g_2, \tau)(t - \tau)^{\kappa-1} d\tau \right\|_\infty, \\ &\leq \frac{1}{\Gamma(\kappa)} \int_0^t \|z_4(f_{11}, f_{21}, f_{31}, f_{41}, g_1, g_2, \tau) - z_4(f_{12}, f_{22}, f_{32}, f_{42}, g_1, g_2, \tau)\|_\infty (t - \tau)^{\kappa-1} d\tau, \\ &\leq \frac{1}{\Gamma(\kappa)} \int_0^t \|-f_{41} + f_{12} + \alpha_3 f_4 + f_{42} - f_{11} + \alpha_3 f_4\|_\infty (t - \tau)^{\kappa-1} d\tau, \\ &\leq \frac{1}{\Gamma(\kappa)} \int_0^t \|f_{42} - f_{41}\|_\infty (t - \tau)^{\kappa-1} d\tau < \frac{1}{\Gamma(\kappa)} \|f_{42} - f_{41}\|_\infty \cdot \frac{\bar{a}^\kappa}{\kappa}, \\ &\leq \frac{\|f_{42} - f_{41}\|_\infty \bar{a}^\kappa}{\Gamma(\kappa+1)} \leq \|f_{42} - f_{41}\|_\infty \gamma_4, \end{aligned} \tag{30}$$

where

$$\gamma_4 = \frac{\bar{a}^\kappa}{\Gamma(\kappa+1)}. \tag{31}$$

For fifth component:

$$\left. \begin{aligned} \|\Lambda_5 g_{11} - \Lambda_5 g_{12}\|_\infty &= \left\| \frac{1}{\Gamma(\kappa)} \int_0^t z_5(f_1, f_2, f_3, f_4, g_{11}, g_2, \tau)(t-\tau)^{\kappa-1} d\tau, \right. \\ &\quad \left. - \frac{1}{\Gamma(\kappa)} \int_0^t z_5(f_1, f_2, f_3, f_4, g_{12}, g_2, \tau)(t-\tau)^{\kappa-1} d\tau \right\|_\infty, \\ &\leq \frac{1}{\Gamma(\kappa)} \int_0^t \|z_5(f_1, f_2, f_3, f_4, g_{11}, g_2, \tau) - z_5(f_1, f_2, f_3, f_4, g_{11}, \\ &\quad g_2, \tau)\|_\infty (t-\tau)^{\kappa-1} d\tau, \\ &\leq \frac{1}{\Gamma(\kappa)} \int_0^t \|-f_{41} + f_1 f_2 + \alpha_3 f_4 + f_{42} - f_1 f_2 + \alpha_3 f_3\|_\infty (t-\tau)^{\kappa-1} d\tau, \\ &\leq \frac{|\alpha_4|}{\Gamma(\kappa)} \int_0^t \|f_{42} - f_{41}\|_\infty (t-\tau)^{\kappa-1} d\tau < \frac{|\alpha_4|}{\Gamma(\kappa)} \|f_{42} - f_{41}\|_\infty \cdot \frac{t^\kappa}{\kappa}, \\ &\leq \frac{|\alpha_4| \|f_{42} - f_{41}\|_\infty \bar{t}^\kappa}{\Gamma(\kappa+1)} \leq |\alpha_4| \|f_{42} - f_{41}\|_\infty \gamma_5, \end{aligned} \right\} \quad (32)$$

where

$$\gamma_5 = \frac{|\alpha_4| \bar{t}^\kappa}{\Gamma(\kappa+1)}. \quad (33)$$

While for the sixth component:

$$\left. \begin{aligned} \|\Lambda_6 g_{21} - \Lambda_6 g_{22}\|_\infty &= \left\| \frac{1}{\Gamma(\kappa)} \int_0^t z_6(f_1, f_2, f_3, f_4, g_1, g_{21}, \tau)(t-\tau)^{\kappa-1} d\tau, \right. \\ &\quad \left. - \frac{1}{\Gamma(\kappa)} \int_0^t z_6(f_1, f_2, f_3, f_4, g_1, g_{22}, \tau)(t-\tau)^{\kappa-1} d\tau \right\|_\infty, \\ &\leq \frac{1}{\Gamma(\kappa)} \int_0^t \|z_6(f_1, f_2, f_3, f_4, g_1, g_{21}, \tau) - z_6(f_1, f_2, f_3, f_4, g_1, \\ &\quad g_{22}, \tau)\|_\infty (t-\tau)^{\kappa-1} d\tau, \\ &\leq \frac{1}{\Gamma(\kappa)} \int_0^t \|- \alpha_4 g_{21} + \alpha_4 g_0^0 - 2\alpha_3 f_3 - 4f_1 f_3 + \alpha_4 g_{22} - \alpha_4 g_2^0 + 2\alpha_3 f_3 \\ &\quad + 4f_1 f_3\|_\infty (t-\tau)^{\kappa-1} d\tau, \\ &\leq \frac{|\alpha_4|}{\Gamma(\kappa)} \int_0^t \|g_{22} - g_{21}\|_\infty (t-\tau)^{\kappa-1} d\tau < \frac{|\alpha_4|}{\Gamma(\kappa)} \|g_{22} - g_{21}\|_\infty \cdot \frac{t^\kappa}{\kappa}, \\ &\leq \frac{|\alpha_4| \|g_{22} - g_{21}\|_\infty \bar{t}^\kappa}{\Gamma(\kappa+1)} \leq |\alpha_4| \|g_{22} - g_{21}\|_\infty \gamma_6, \end{aligned} \right\} \quad (34)$$

where

$$\gamma_6 = \frac{|\alpha_4| \bar{t}^\kappa}{\Gamma(\kappa+1)}. \quad (35)$$

So, Λ is a contraction if

$$\begin{pmatrix} \gamma_1 \\ \gamma_2 \\ \gamma_3 \\ \gamma_4 \\ \gamma_5 \\ \gamma_6 \end{pmatrix} < \begin{pmatrix} 1 \\ 1 \\ 1 \\ 1 \\ 1 \\ 1 \end{pmatrix} = 0, \quad (36)$$

for

$$\begin{aligned} \bar{a} &< \left(\frac{\Gamma(\kappa+1)}{|\alpha_1|} \right)^{\frac{1}{\kappa}}, \quad \bar{a} < \Gamma(\kappa+1)^{\frac{1}{\kappa}}, \quad \bar{a} < \Gamma(\kappa+1)^{\frac{1}{\kappa}}, \\ \bar{a} &< \Gamma(\kappa+1)^{\frac{1}{\kappa}}, \quad \bar{a} < \left(\frac{\Gamma(\kappa+1)}{|\alpha_4|} \right)^{\frac{1}{\kappa}}, \quad \text{and} \quad \bar{a} < \left(\frac{\Gamma(\kappa+1)}{|\alpha_4|} \right)^{\frac{1}{\kappa}}. \end{aligned}$$

So to obtain a contraction

$$\bar{a} = \min \left\{ \begin{array}{l} \left(\frac{\Gamma(\kappa+1)}{|\alpha_1|} \right)^{\frac{1}{\kappa}}, \quad \Gamma(\kappa+1)^{\frac{1}{\kappa}}, \quad \Gamma(\kappa+1)^{\frac{1}{\kappa}}, \\ \Gamma(\kappa+1)^{\frac{1}{\kappa}}, \quad \left(\frac{\Gamma(\kappa+1)}{|\alpha_4|} \right)^{\frac{1}{\kappa}}, \quad \left(\frac{\Gamma(\kappa+1)}{|\alpha_4|} \right)^{\frac{1}{\kappa}}, \end{array} \right\}. \quad (37)$$

Γ is a contraction in a Banach space under this condition, which implies that Γ has a unique solution. Readers are directed to some famous publications for the broad existence and uniqueness theorem in [7,8,13].

4. Numerical Scheme

Here, to avoid confusion we address the symbols $f_1, f_2, f_3, f_4, g_1, g_2$, as $f^{(1)}, f^{(2)}, f^{(3)}, f^{(4)}, g^{(1)}, g^{(2)}$, such that the resultant Adams Bashforth Scheme becomes:

$$\begin{aligned} f^{(1)}(t_{q+1}) &= f^{(1)}(t_q) + \frac{\varphi(t_q, f_q^{(1)})}{h\Gamma(\kappa)} \left\{ \frac{2h}{\kappa} t_q^\kappa - \frac{t_q^{\kappa+1}}{\kappa+1} + \frac{h}{\kappa} t_q^\kappa - \frac{t_q^{\kappa+1}}{\kappa} \right\} \\ &\quad + \frac{\varphi(t_{q-1}, f_{q-1}^{(1)})}{h\Gamma(\kappa)} \left\{ \frac{h}{\kappa} t_{q+1}^\kappa - \frac{t_{q+1}^{\kappa+1}}{\kappa+1} + \frac{t_q^\kappa}{\kappa+1} \right\}. \end{aligned} \quad (38)$$

$$\begin{aligned} f^{(2)}(t_{q+1}) &= f^{(2)}(t_q) + \frac{\varphi(t_q, f_q^{(2)})}{h\Gamma(\kappa)} \left\{ \frac{2h}{\kappa} t_q^\kappa - \frac{t_q^{\kappa+1}}{\kappa+1} + \frac{h}{\kappa} t_q^\kappa - \frac{t_q^{\kappa+1}}{\kappa} \right\} \\ &\quad + \frac{\varphi(t_{q-1}, f_{q-1}^{(2)})}{h\Gamma(\kappa)} \left\{ \frac{h}{\kappa} t_{q+1}^\kappa - \frac{t_{q+1}^{\kappa+1}}{\kappa+1} + \frac{t_q^\kappa}{\kappa+1} \right\}. \end{aligned} \quad (39)$$

$$\begin{aligned} f^{(3)}(t_{q+1}) &= f^{(3)}(t_q) + \frac{\varphi(t_q, f_q^{(3)})}{h\Gamma(\kappa)} \left\{ \frac{2h}{\kappa} t_q^\kappa - \frac{t_q^{\kappa+1}}{\kappa+1} + \frac{h}{\kappa} t_q^\kappa - \frac{t_q^{\kappa+1}}{\kappa} \right\} \\ &\quad + \frac{\varphi(t_{q-1}, f_{q-1}^{(3)})}{h\Gamma(\kappa)} \left\{ \frac{h}{\kappa} t_{q+1}^\kappa - \frac{t_{q+1}^{\kappa+1}}{\kappa+1} + \frac{t_q^\kappa}{\kappa+1} \right\}. \end{aligned} \quad (40)$$

$$\begin{aligned} f^{(4)}(t_{q+1}) &= f^{(4)}(t_q) + \frac{\varphi(t_q, f_q^{(4)})}{h\Gamma(\kappa)} \left\{ \frac{2h}{\kappa} t_q^\kappa - \frac{t_q^{\kappa+1}}{\kappa+1} + \frac{h}{\kappa} t_q^\kappa - \frac{t_q^{\kappa+1}}{\kappa} \right\} \\ &\quad + \frac{\varphi(t_{q-1}, f_{q-1}^{(4)})}{h\Gamma(\kappa)} \left\{ \frac{h}{\kappa} t_{q+1}^\kappa - \frac{t_{q+1}^{\kappa+1}}{\kappa+1} + \frac{t_q^\kappa}{\kappa+1} \right\}. \end{aligned} \quad (41)$$

$$\begin{aligned} g^{(1)}(t_{q+1}) &= g_1(t_q) + \frac{\varphi(t_q, g_q^{(1)})}{h\Gamma(\kappa)} \left\{ \frac{2h}{\kappa} t_q^\kappa - \frac{t_q^{\kappa+1}}{\kappa+1} + \frac{h}{\kappa} t_q^\kappa - \frac{t_q^{\kappa+1}}{\kappa} \right\} \\ &\quad + \frac{\varphi(t_{q-1}, g_{q-1}^{(1)})}{h\Gamma(\kappa)} \left\{ \frac{h}{\kappa} t_{q+1}^\kappa - \frac{t_{q+1}^{\kappa+1}}{\kappa+1} + \frac{t_q^\kappa}{\kappa+1} \right\}. \end{aligned} \quad (42)$$

$$\begin{aligned} g^{(2)}(t_{q+1}) &= g^{(2)}(t_q) + \frac{\varphi(t_q, g_q^{(2)})}{h\Gamma(\kappa)} \left\{ \frac{2h}{\kappa} t_q^\kappa - \frac{t_q^{\kappa+1}}{\kappa+1} + \frac{h}{\kappa} t_q^\kappa - \frac{t_q^{\kappa+1}}{\kappa} \right\} \\ &\quad + \frac{\varphi(t_{q-1}, g_{q-1}^{(2)})}{h\Gamma(\kappa)} \left\{ \frac{h}{\kappa} t_{q+1}^\kappa - \frac{t_{q+1}^{\kappa+1}}{\kappa+1} + \frac{t_q^\kappa}{\kappa+1} \right\}. \end{aligned} \quad (43)$$

5. Clustering by K-Means Algorithm

We categorize the sample pattern congregation $\{V\} = \{V_1, V_2, V_3, \dots, V_N\}$ into C classes, which are $P_1, P_2, P_3, \dots, P_c, M_k$ and P_k mean vectors. So:

$$M_k = \frac{1}{N_k} \sum_{V \in P_k} V, \quad N_k = |P_k|. \quad (44)$$

By definition of cluster criterion function as below:

$$G = \sum_{k=1}^c \sum_{V \in P_k} \|V - M_k\|^2, \quad (45)$$

where, N_k and P_k are the number of samples and G is the quadratic sum of all types of sample classes' inaccuracy and their mean value. It's also known as the sum of sample distances and their mean value. As a result, we should make every effort to obtain the lowest possible value discussed in [13].

5.1. Clustering algorithm

To classify the patterns of N quantity of samples which are $\{v_1, v_2, v_3, \dots, v_N\}$, into J clusters: we follow the steps given below.

- Step. 1 To choose the first cluster focal point. For instance, we choose $u_1 = v_1$ among $\{v_1, v_2, v_3, \dots, v_N\}$.
- Step. 2 Choose a new focus point for the second cluster that is as far away from u_1 as feasible, and measure the distance between each sample and $u_1 : \|v_k - u_1\|, k = 1, 2, \dots, N$. If: $\|v_h - u_1\| = \max\{\|v_k - u_1\|, k = 1, 2, \dots, N\}$, $h = 1, 2, \dots, N$. Thus, the second cluster we choose v_h to be the focal point, and $u_2 = v_h$.
- Step. 3 Measuring the norm between samples $\{v_1, v_2, v_3, \dots, v_N\}$ and focal points $\{u_1, u_2\}$, respectively, such that $d_{k1} = \|v_k - u_1\|, k = 1, 2, \dots, N$, $d_{k2} = \|v_k - u_2\|, k = 1, 2, \dots, N$. Take a minimum of the outcomes is given by: $\min(d_{k1}, d_{k2}), k = 1, 2, \dots, N$ and combine all the focal points $\{v_1, u_2\}$ and the minimums of all samples of pattern. For the third focal point u_3 , take the maximum from minimum of the outcomes. If: $\min(d_{h1}, d_{h2}) = \max\{\min(d_{k1}, d_{k2}), k = 1, 2, 3, \dots, N\}$, $h = 1, 2, 3, \dots, N$.
- Step. 4 Let, we obtained $\{u_k, k = 1, 2, 3, \dots, s\}$ cluster focal points of $s(s < j)$, further we need to determine the $(r + 1)$ th cluster focal point, namely if: $\min(d_{h1}, d_{h2}, \dots, d_{hs}) = \max\{\min(d_{h1}, d_{h2}, \dots, d_{hs}), k = 1, 2, 3, \dots, N\}$ $h = 1, 2, \dots, N$, then: $u_{s+1} = v_h$.
- Step.5 Repeat the process till $s + 1 = j$.
- Step. 6 Now we have chosen J initial cluster focal point $u_1(1), u_2(1), u_3(1), \dots, u_j(1)$. Where, the numbers in parenthesis are indices of iterations.
- Step. 7 Allocate $\{v_1, v_2, v_3, \dots, v_N\}$ to one of the J clusters, and minimize the distance we have $\|v - u_h(t)\| = \min\{\|v - u_k(t)\|, k = 1, 2, 3, \dots, J\}$, $h = 1, 2, 3, \dots, J$ Then: $v \in s_j(t)$. The symbol t in the formula is the serial number of iterative operations, s_j stands for the j th cluster, and the cluster focal point is u_j .
- Step. 8 Measure the values of new vector to all cluster focal point such that $u_h(t + 1), h = 1, 2, 3, \dots, J$, the means vectors of all clusters samples that is $u_h(t + 1) = \frac{1}{N_h} \sum_{v \in s_j(t)} v, h = 1, 2, \dots, J$, where N_h is the number of samples of the h th cluster s_h and next measuring the J samples of clusters. Making mean vectors be new clusters can minimize cluster criterion function J_j such that: $J_h = \sum_{v \in s_h(t)} \|v - u_h(t + 1)\|^2, h = 1, 2, \dots, J$.
- Step. 9 Eventually, if $u_h(t + 1) = u_h(t), h = 1, 2, \dots, J$, then the convergence of the algorithm is finished while repeat the process from **Step.7** if $u_h(t + 1) \neq u_h(t), h = 1, 2, 3, \dots, J$.

6. Results and Discussion

Combining the numerical scheme and the clustering algorithm, the results are obtained by using the values given in the following **Table 1** and **Table 2**:

The entire experiment clustered the data in 0.259274 s for each figure with a difference $h = 0.001$. Applied the K-mean algorithm to the data of solution of the model after obtaining the results from the numerical scheme for each class to organize the data into ten clusters. Then, by the programming manipulation, the solutions have been colored and associated with each cluster. To show possible dynamics and trajectory of solutions of the model (2) we present the results in 2D and 3D. The **Figs. 1–6** shows the trajectory of f_1 the Rabi flopping quantity representing the electric field amplitude at emission frequency, f_2 the normalized density matrix element, f_3 the normalized density matrix element, f_4 the normalized density matrix element, g_1 the population difference, and g_2 the population difference with a classical order $\kappa = 1$, respectively. The **Figs. 7–12** show the trajectories with a fractional order $\kappa = 0.88$ of solutions f_1 the Rabi flopping quantity representing the electric field amplitude at emission frequency, f_2 the normalized density matrix element, f_3 the normalized density matrix element, f_4 the normalized density matrix element, g_1 the population difference, and g_2 the population difference. In **Figs. 13–22** the 2D plot show the trajectories of two class vs. class while in **Figs. 23–28** the 3D trajectories have been showed. The programming has been done throughout the MATLAB environment and used the numerical data of the solution to the model (2) and the MATLAB code for clustering and the numerical scheme has been combined. Here we compare the CPU time for the proposed method with that of the RK4 method in **Table 3** by using MATLAB 13 and Machine Cori-7 of HP with 8th generation. Here we see as the order is enlarging the CPU time is reducing and also as compared to RK4 the proposed method is less expensive in time. For small

Table 1 Table of description compartments of variables with initial conditions.

Class	Initial Condition	Class	Initial Conditions	Class	Initial Condition
$f_1(t)$	1	$f_2(t)$	1	$f_3(t)$	1
$f_4(t)$	1	$g_1(t)$	1	$g_2(t)$	1

Table 2 Table of description and values of parameters.

Parameter	Value	Parameter	Value	Parameter	Value
α_1	1.5	α_2	50	α_3	3.8
α_4	0.43858	N_1^0	1	N_2^0	1.8

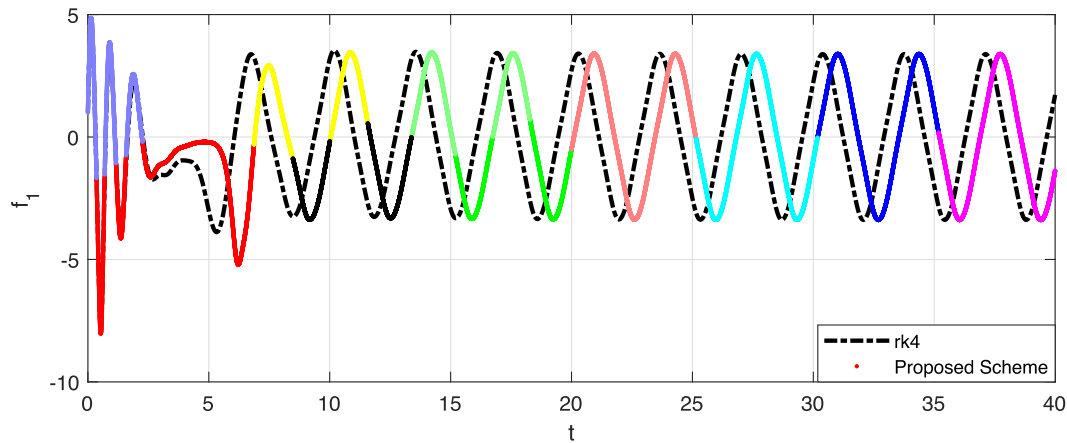


Fig. 1 The dynamics of strange attractor, f_1 the Rabi flopping quantity representing the electric field amplitude at emission frequency for the classical case with order $\kappa = 1$. While it shows the comparison of RK4 and proposed scheme..

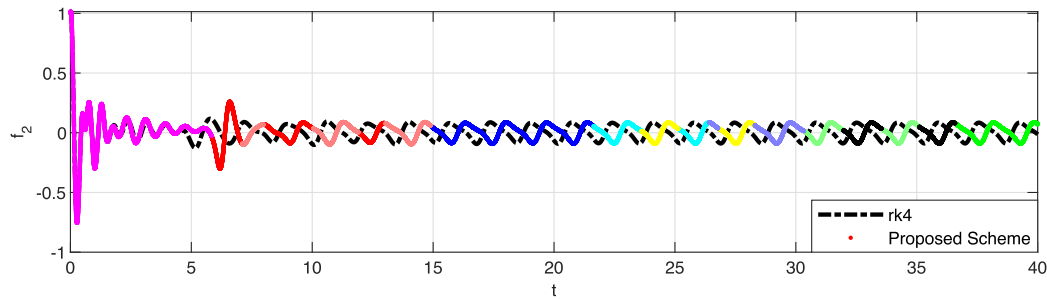


Fig. 2 The dynamics of strange attractor, f_2 is the normalized density matrix element for the classical case with order $\kappa = 1$. While it shows the comparison of RK4 and proposed scheme..

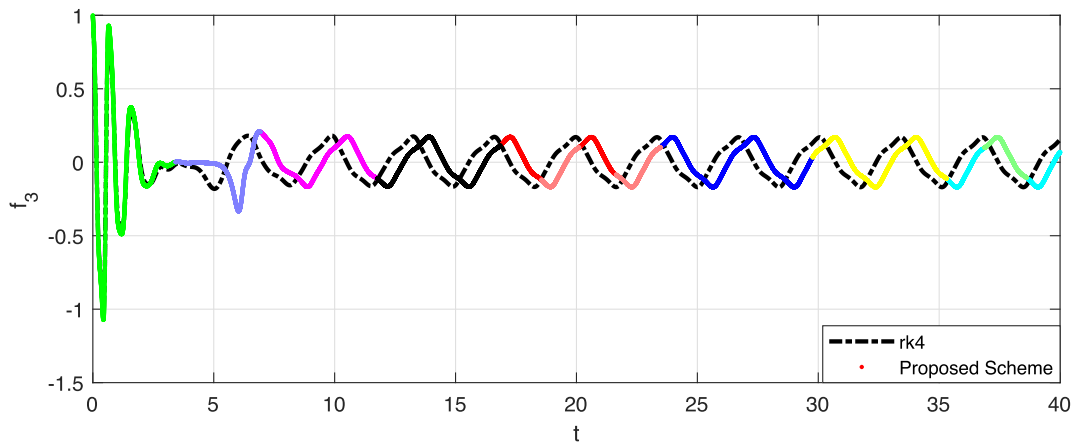


Fig. 3 The dynamics of strange attractor, f_3 is the normalized density matrix element for the classical case with order $\kappa = 1$. While it shows the comparison of RK4 and proposed scheme..

fractional order larger time indicates the complexity in fractional order. This will take more time to resolve as compared to integer order.

From Table 4, we conclude that cluster plays important role in reducing CPU time. Further, K-means clustering algo-

rithm is one of the most commonly used procedure which has diverse scope for implementation. The mentioned algorithm has important applications in the signal and image processing, artificial intelligence and many other fields. Further, we remark that clustering is one of the most significant applica-

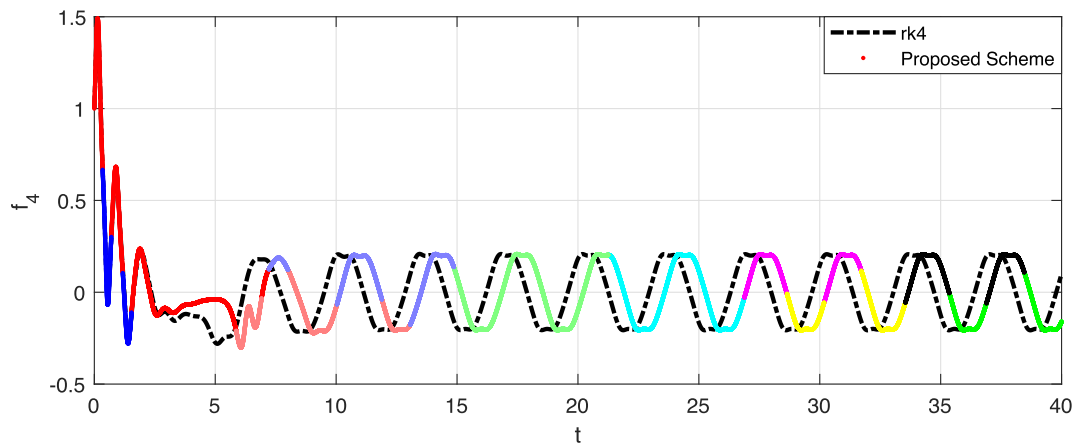


Fig. 4 The dynamics of strange attractor, f_4 is the normalized density matrix element for the classical case with order $\kappa = 1$. While it shows the comparison of RK4 and proposed scheme..

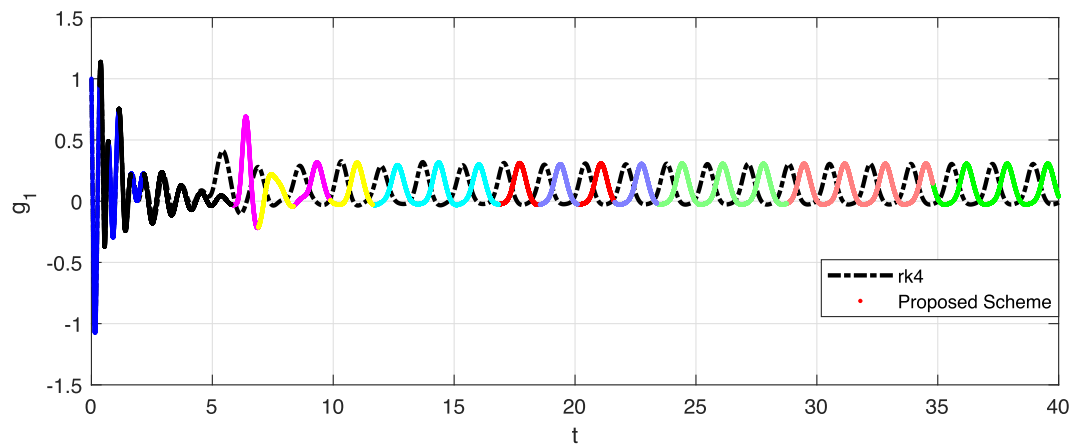


Fig. 5 The dynamics of strange attractor, g_1 the population difference for the classical case with order $\kappa = 1$. While it shows the comparison of RK4 and proposed scheme..

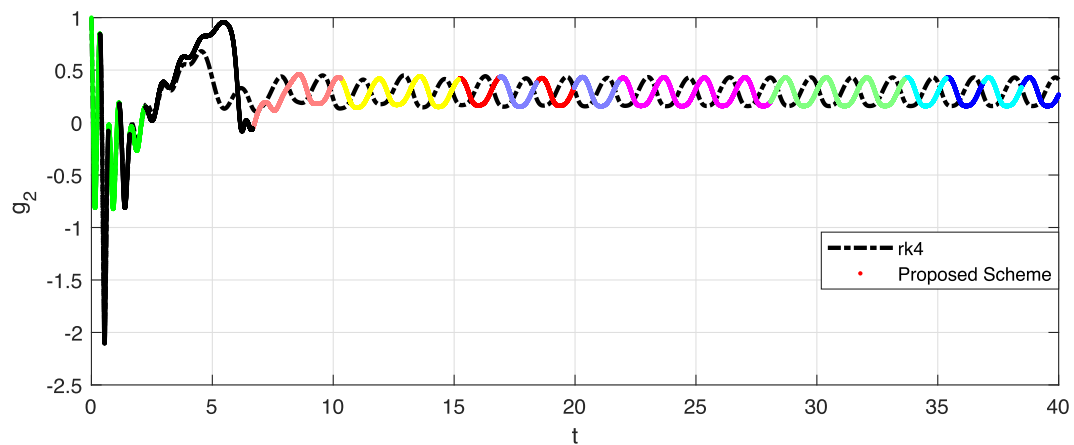


Fig. 6 The dynamics of strange attractor, g_2 the population difference for the classical case with order $\kappa = 1$. While it shows the comparison of RK4 and proposed scheme..

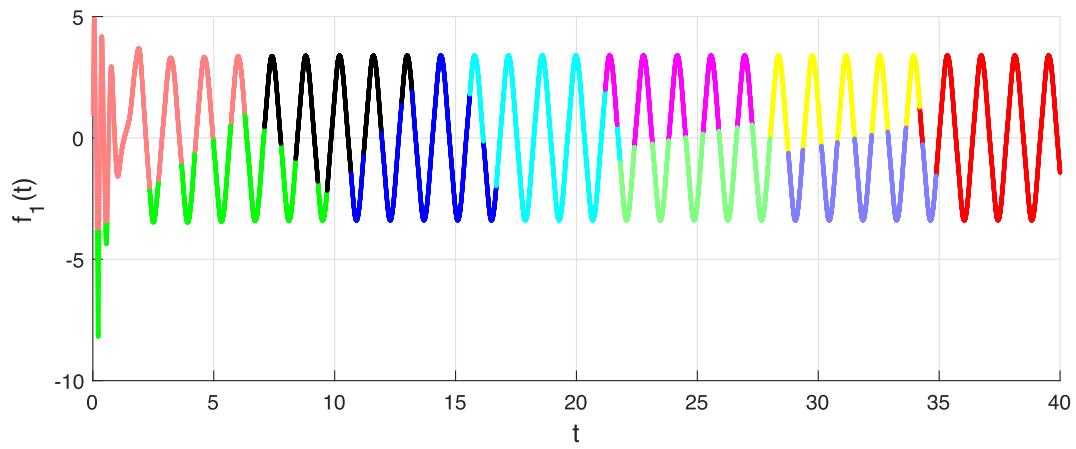


Fig. 7 The dynamics of strange attractor, f_1 the Rabi flopping quantity representing the electric field amplitude at emission frequency for the Fractional case with order $\kappa = 0.88$.

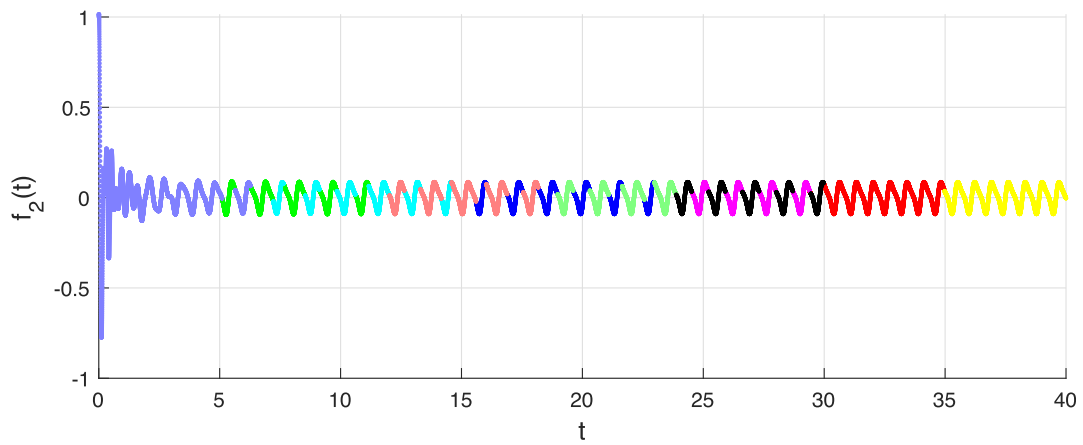


Fig. 8 The dynamics of strange attractor, f_2 is the normalized density matrix element for the Fractional case with order $\kappa = 0.88$.

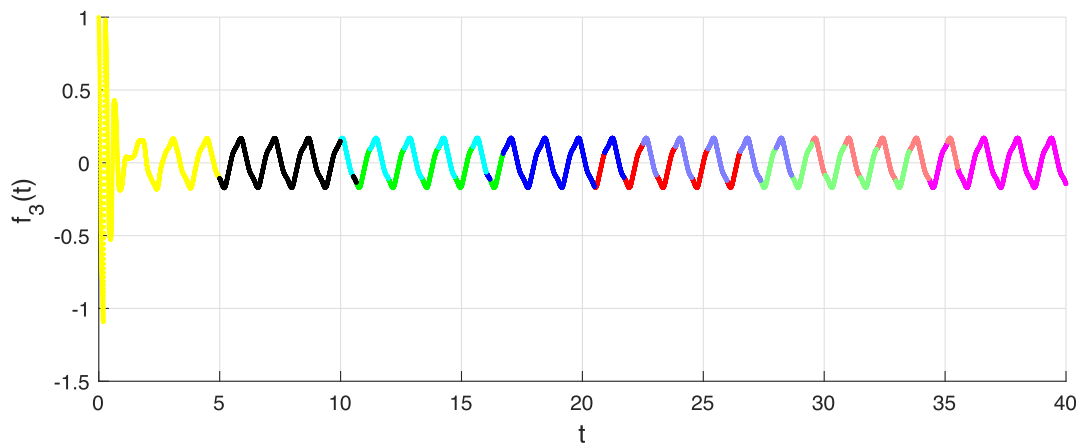


Fig. 9 The dynamics of strange attractor, f_3 is the normalized density matrix element for the Fractional case with order $\kappa = 0.88$.

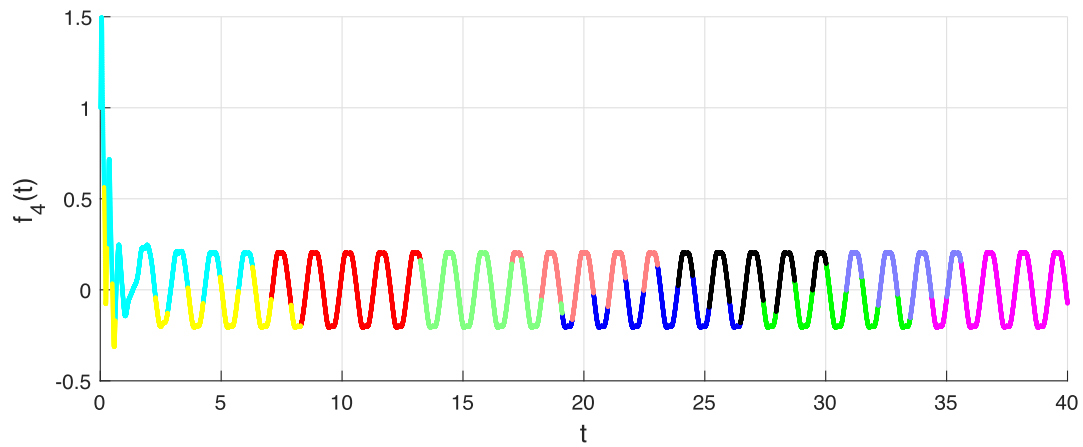


Fig. 10 The dynamics of strange attractor, f_4 is the normalized density matrix element for the Fractional case with order $\kappa = 0.88$.

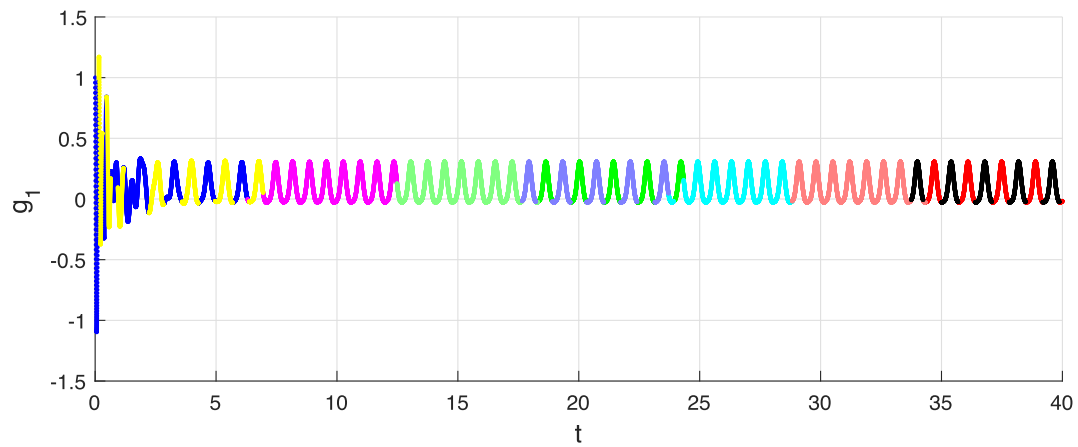


Fig. 11 The dynamics of strange attractor, g_1 the population difference for the Fractional case with order $\kappa = 0.88$.

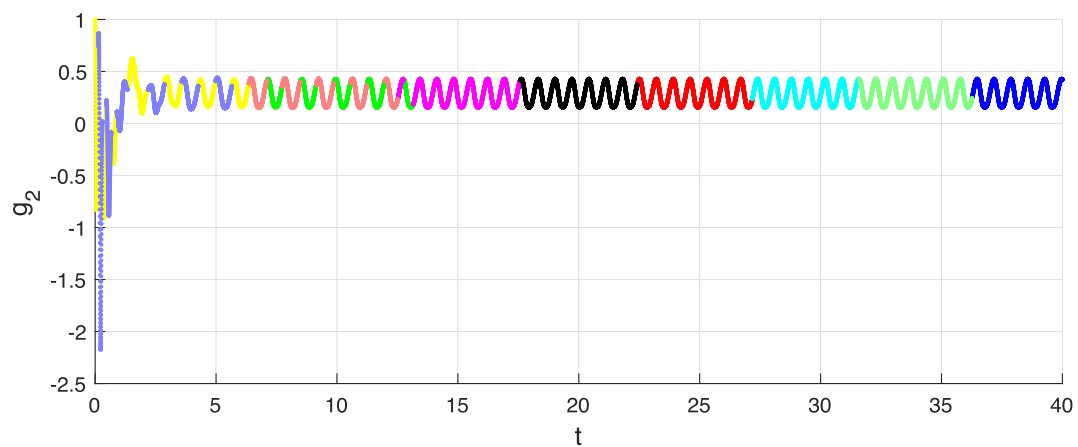


Fig. 12 The dynamics of strange attractor, g_2 the population difference for the Fractional case with order $\kappa = 0.88$.

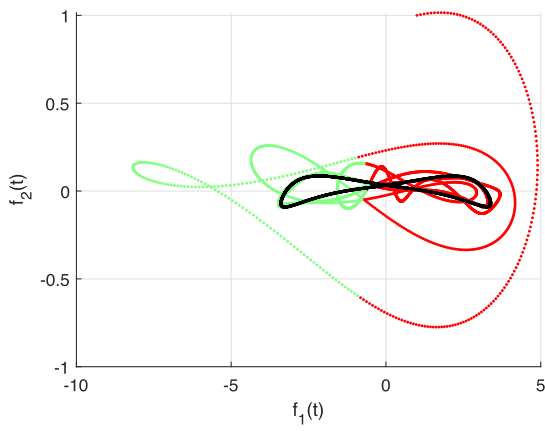


Fig. 13 The dynamics of strange attractors, f_1 the Rabi flopping quantity representing the electric field amplitude at emission frequency vs. f_2 is the normalized density matrix element for the Fractional case with order $\kappa = 0.88$.

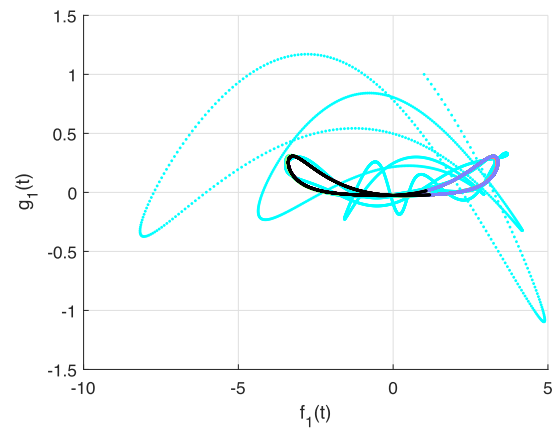


Fig. 16 The dynamics of strange attractors, f_1 the Rabi flopping quantity representing the electric field amplitude at emission frequency vs. g_1 the population difference for the Fractional case with order $\kappa = 0.88$.

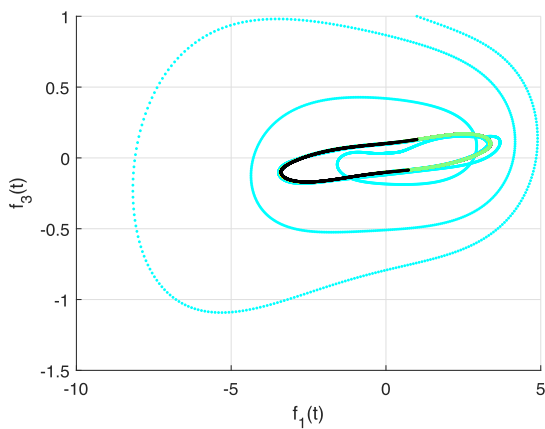


Fig. 14 The dynamics of strange attractors, f_1 the Rabi flopping quantity representing the electric field amplitude at emission frequency vs. f_3 is the normalized density matrix element for the Fractional case with order $\kappa = 0.88$.

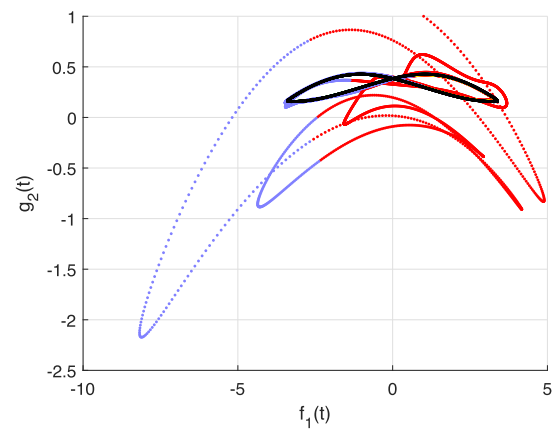


Fig. 17 The dynamics of strange attractors, f_1 the Rabi flopping quantity representing the electric field amplitude at emission frequency vs. g_2 the population difference for the Fractional case with order $\kappa = 0.88$.

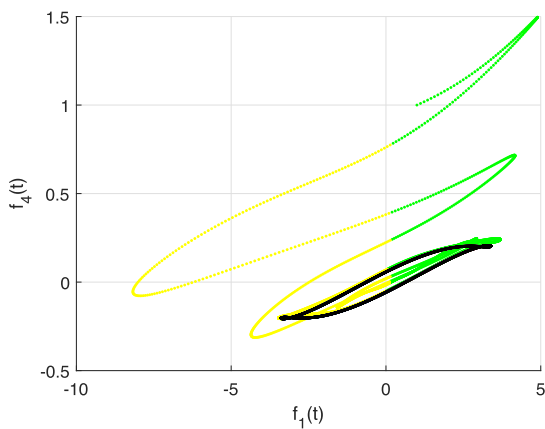


Fig. 15 The dynamics of strange attractors, f_1 the Rabi flopping quantity representing the electric field amplitude at emission frequency vs. f_4 is the normalized density matrix element for the Fractional case with order $\kappa = 0.88$.

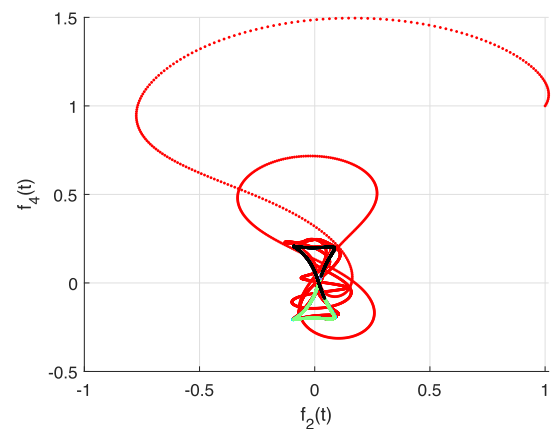


Fig. 18 The dynamics of strange attractor, f_2 is the normalized density matrix element vs. f_4 is the normalized density matrix element for the Fractional case with order $\kappa = 0.88$.

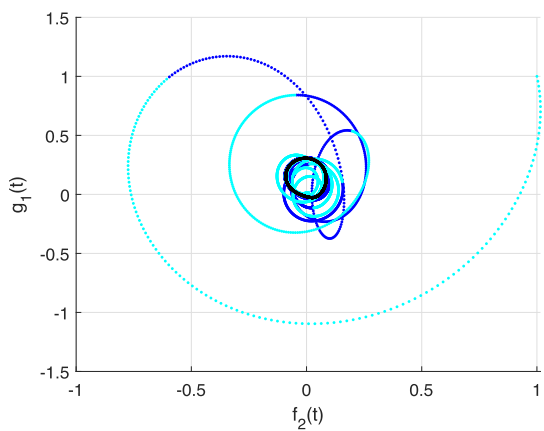


Fig. 19 The dynamics of strange attractor, f_2 is the normalized density matrix element vs. g_1 the population difference for the Fractional case with order $\kappa = 0.88$.

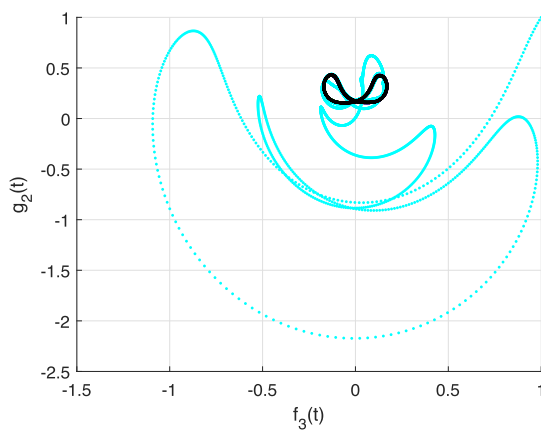


Fig. 22 The dynamics of strange attractor, f_3 is the normalized density matrix element vs. g_2 the population difference for the Fractional case with order $\kappa = 0.88$.

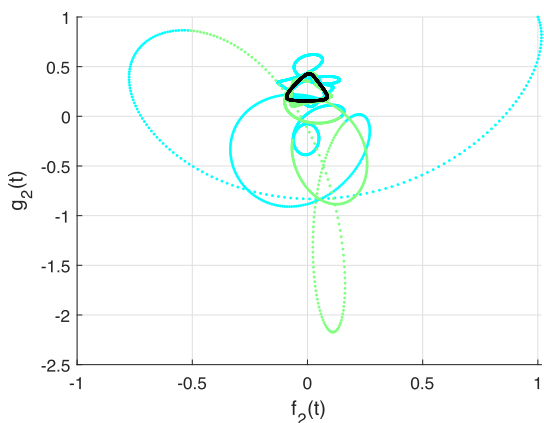


Fig. 20 The dynamics of strange attractor, f_2 is the normalized density matrix element vs. g_2 the population difference for the Fractional case with order $\kappa = 0.88$.

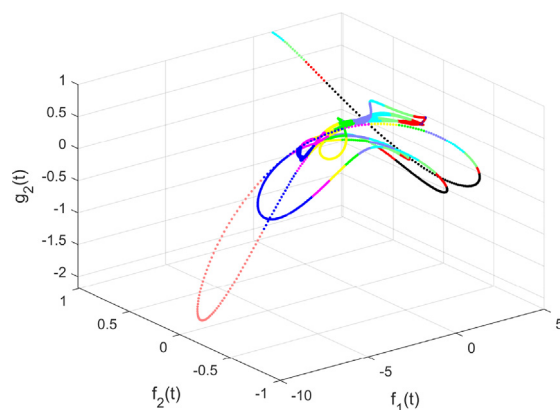


Fig. 23 The dynamics of strange attractors, f_1 the Rabi flopping quantity representing the electric field amplitude at emission frequency vs. f_2 is the normalized density matrix element vs. g_2 the population difference for the Fractional case with order $\kappa = 0.88$.

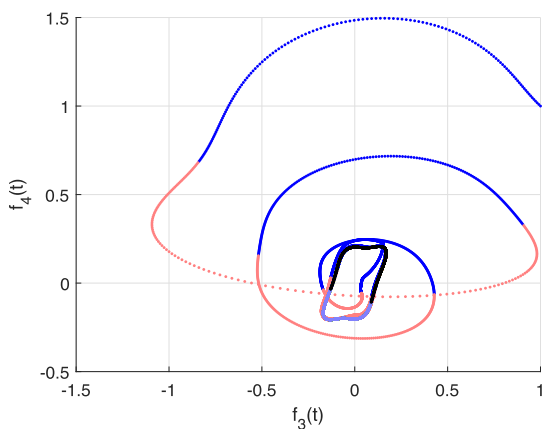


Fig. 21 The dynamics of strange attractor, f_3 is the normalized density matrix element vs. f_4 is the normalized density matrix element for the Fractional case with order $\kappa = 0.88$.

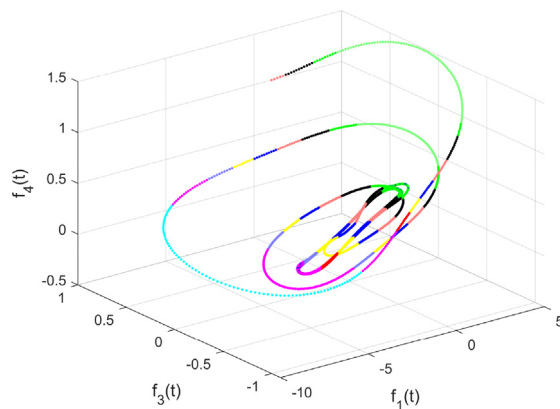


Fig. 24 The dynamics of strange attractors, f_1 the Rabi flopping quantity representing the electric field amplitude at emission frequency vs. f_3 is the normalized density matrix element vs. f_4 is the normalized density matrix element for the Fractional case with order $\kappa = 0.88$.

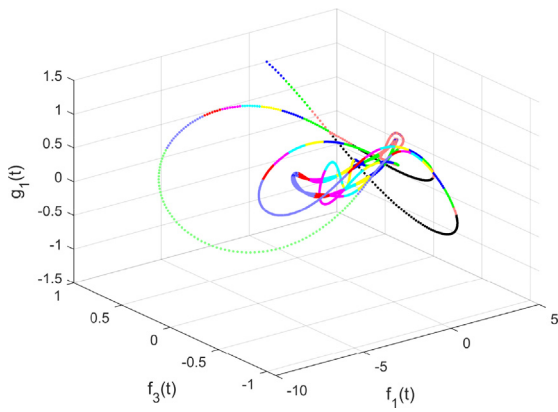


Fig. 25 The dynamics of strange attractors, f_1 the Rabi flopping quantity representing the electric field amplitude at emission frequency vs. f_3 is the normalized density matrix element vs. g_1 the population difference for the Fractional case with order $\kappa = 0.88$.

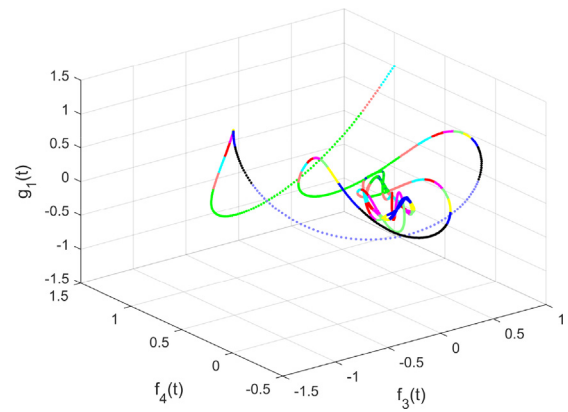


Fig. 28 The dynamics of strange attractors, f_3 is the normalized density matrix element vs. f_4 is the normalized density matrix element vs. g_1 the population difference for the Fractional case with order $\kappa = 0.88$.

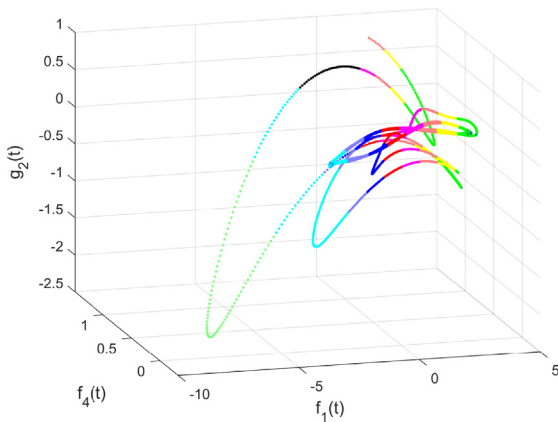


Fig. 26 The dynamics of strange attractors, f_1 the Rabi flopping quantity representing the electric field amplitude at emission frequency vs. f_4 is the normalized density matrix element vs. g_2 the population difference for the Fractional case with order $\kappa = 0.88$.

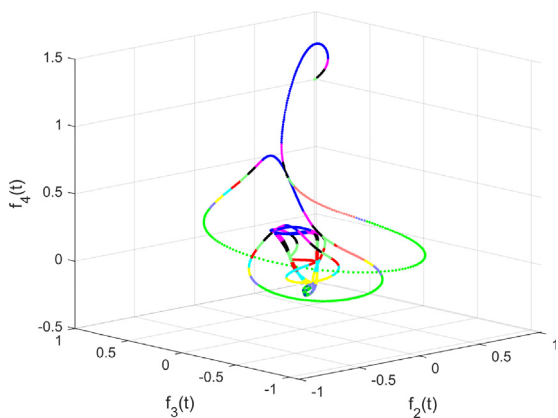


Fig. 27 The dynamics of strange attractors, f_2 is the normalized density matrix element vs. f_3 is the normalized density matrix element vs. f_4 is the normalized density matrix element for the Fractional case with order $\kappa = 0.88$.

Table 3 Comparison of CPU time of the proposed and RK4 method for the considered model.

Fractional order κ	CPU time of the Proposed method in seconds	CPU time of RK4 method in seconds
0.50	55	57
0.60	53	56
0.70	49	51
0.80	45	47
0.90	44	45
1.00	30	33

Table 4 Comparison of CPU time of the proposed method for the considered model with and without clustering at the order $\kappa = 1$.

Clusters	CPU time with cluster in seconds	CPU time without cluster in seconds
10	0.0010	0.0090
20	0.0050	0.0180
30	0.0070	0.0340
45	0.0180	0.0380
60	0.0200	0.0510
75	0.0390	0.0540

tions in the big data field. The CPU time performance of the aforesaid technique is much better with clustering for numerical data as compared to categorical data.

7. Conclusion

In this work, a fractional sixth order laser model of a resonant which has been homogeneously extended three levels optically pumped has been investigated. The concerned investigation has been based on the detection of different chaotic behaviors

of the proposed model and its existence theory. For the statistical analysis, we have used an advanced clustering method based on the K-Means algorithm and the Adam Bashforth scheme. We have presented different chaotic behaviors of the dynamics of various compartments corresponding to various fractional orders. In addition, before the numerical investigation, we presented a massive existence analysis and uniqueness of solutions to the proposed problems by using the Banach contraction theorem and other tools of nonlinear analysis. The goal of the “k-means clustering” is to divide a set of n observations into k groups, with each observation belonging to the cluster represented by its nearest mean. The data space is then divided into Thiessen polygons as a result of this. Therefore, each color belongs to a different cluster in all figures. The proposed algorithm has many applications in real life, such as medical imaging segmentation, search engines, and wireless sensor networks. For identifying the cluster heads that gather all the data for each cluster and many more. A comparison of the proposed scheme and the Runge–Kutta scheme is also presented. Finally, a comparison with the RK4 method in CPU time has been given. We see that the proposed method is less expensive in time as compared to the traditional RK4 method. In the future, the aforementioned consideration model can be studied under non-singular and fractal-fractional type derivatives for more results.

Declaration of Competing Interest

The authors declare that they have no known competing financial interests or personal relationships that could have appeared to influence the work reported in this paper.

Acknowledgement

The authors Kamal Shah and Thabet Abdeljawad would like to thank Prince Sultan University for paying the APC and support through the TAS research lab.

References

- [1] J. v. Moloney, W. Forysiak, J.S. Uppal, R.G. Harrison, Regular and chaotic dynamics of optically pumped molecular lasers, *Phys. Rev. A*. 39 (1989) 1277–1285. <https://doi.org/10.1103/PhysRevA.39.1277>.
- [2] W. Forysiak, J.V. Moloney, R.G. Harrison, Bifurcations of an optically pumped three-level laser model, *Physica D: Nonlinear Phenomena*. 53 (1991) 162–186, [https://doi.org/10.1016/0167-2789\(91\)90170-E](https://doi.org/10.1016/0167-2789(91)90170-E).
- [3] K. Pusuluri, H.G.E. Meijer, A.L. Shilnikov, (INVITED) Homoclinic puzzles and chaos in a nonlinear laser model, *Commun. Nonlinear Sci. Numer. Simul.* 93 (2021) 105503, <https://doi.org/10.1016/j.cnsns.2020.105503>.
- [4] Y. Li, H. Wu, A clustering method based on K-means algorithm, *Phys. Proc.* 25 (2012) 1104–1109, <https://doi.org/10.1016/J.PHPRO.2012.03.206>.
- [5] B.D. Hassard, B.D. Hassard, N.D. Kazarinoff, Y.H. Wan, Y. W. Wan, *Theory and applications of Hopf bifurcation*, Vol. 41, CUP Archive, 1981.
- [6] Z. Ahmad, F. Ali, N. Khan, I. Khan, Dynamics of fractal-fractional model of a new chaotic system of integrated circuit with Mittag-Leffler kernel, *Chaos, Solitons & Fractals*. 153 (2021) 111602, <https://doi.org/10.1016/J.CHAOS.2021.111602>.
- [7] K. Diethelm, *The Analysis of Fractional Differential Equations*, Springer, Berlin Heidelberg, Berlin, Heidelberg, 2010, pp. 1–30, <https://doi.org/10.1007/978-3-642-14574-2>.
- [8] I. Podlubny, *Fractional Differential Equations (An Introduction to Fractional Derivatives, Fractional Differential Equations, to Methods of Their Solution and Some of Their Applications)*, Academic Press, 1998.
- [9] K.M. Owolabi, A. Atangana, *Numerical Methods for Fractional Differentiation* 54 (2019), <https://doi.org/10.1007/978-981-15-0098-5>.
- [10] Atangana Abdon, Application of Fractional Calculus to Epidemiology, in: *Fractional Dynamics*, De Gruyter Open Poland, 2015: pp. 174–190. doi: 10.1515/9783110472097-011.
- [11] E. Kaiser, B.R. Noack, L. Cordier, A. Spohn, M. Segond, M. Abel, G. Daviller, J. Östh, S. Krajnović, R.K. Niven, Cluster-based reduced-order modelling of a mixing layer, *J. Fluid Mech.* 754 (2014) 365–414, <https://doi.org/10.1017/jfm.2014.355>.
- [12] S.Z. Selim, M.A. Ismail, K-means-type algorithms: a generalized convergence theorem and characterization of local optimality, *IEEE Trans. Pattern Anal. Mach. Intell. PAMI-6* (1984) 81–87, <https://doi.org/10.1109/TPAMI.1984.4767478>.
- [13] M.E. Celebi, H.A. Kingravi, P.A. Vela, A comparative study of efficient initialization methods for the k-means clustering algorithm, *Expert Syst. Appl.* 40 (1) (2013) 200–210.
- [14] A. Atangana, S. Qureshi, Modeling attractors of chaotic dynamical systems with fractal–fractional operators, *Chaos, Solitons & Fractals*. 123 (2019) 320–337, <https://doi.org/10.1016/j.chaos.2019.04.020>.
- [15] D. Baleanu, R.L. Magin, S. Bhalekar, V. Daftardar-Gejji, Chaos in the fractional order nonlinear Bloch equation with delay, *Commun. Nonlinear Sci. Numer. Simul.* 25 (2015) 41–49, <https://doi.org/10.1016/j.cnsns.2015.01.004>.
- [16] G.-C. Wu, D. Baleanu, H.-P. Xie, F.-L. Chen, Chaos synchronization of fractional chaotic maps based on the stability condition, *Physica A: Stat. Mech. Its Appl.* 460 (2016) 374–383, <https://doi.org/10.1016/j.physa.2016.05.045>.
- [17] S. Boccaletti, J. Kurths, G. Osipov, D.L. Valladares, C.S. Zhou, The synchronization of chaotic systems, *Phys. Rep.* 366 (2002) 1–101, [https://doi.org/10.1016/S0370-1573\(02\)00137-0](https://doi.org/10.1016/S0370-1573(02)00137-0).
- [18] V.-T. Pham, S. Jafari, T. Kapitaniak, C. Volos, S.T. Kingni, Generating a chaotic system with one stable equilibrium, *Int. J. Bifur. and Chaos*. 27 (2017) 1750053, <https://doi.org/10.1142/S0218127417500535>.
- [19] R.A. Haraty, M. Dimishkieh, M. Masud, An enhanced k - means clustering algorithm for pattern discovery in healthcare data, *Int. J. Distrib. Sensor Networks*. 11 (2015) 615740, <https://doi.org/10.1155/2015/615740>.
- [20] S. Boccaletti, J. Kurths, G. Osipov, D.L. Valladares, C.S. Zhou, The synchronization of chaotic systems, *Phys. Rep.* 366 (2002) 1–101, [https://doi.org/10.1016/S0370-1573\(02\)00137-0](https://doi.org/10.1016/S0370-1573(02)00137-0).
- [21] Saleh AA. Healthcare E-Guide System using K-means Clustering Algorithm Case Study (Healthcare Centers in Khartoum-State) (Doctoral dissertation, Sudan University of Science & Technology).
- [22] R.W. Grant, J. McCloskey, M. Hatfield, C. Uratsu, J.D. Ralston, E. Bayliss, C.J. Kennedy, Use of latent class analysis and k-means clustering to identify complex patient profiles, *JAMA Network Open*. 3 (2020), <https://doi.org/10.1001/JAMANETWORKOPEN.2020.29068>, e2029068–e2029068.
- [23] D. Baleanu, M. Hassan Abadi, A. Jajarmi, K. Zarghami Vahid, J.J. Nieto, A new comparative study on the general fractional model of COVID-19 with isolation and quarantine effects, *Alexandria Eng. J.* 61 (2022) 4779–4791, <https://doi.org/10.1016/j.aej.2021.10.030>.
- [24] V.S. Erturk, E. Godwe, D. Baleanu, P. Kumar, J. Asad, A. Jajarmi, Novel Fractional-Order Lagrangian to Describe

- Motion of Beam on Nanowire, *Acta Physica Polonica A*. 140 (2021) 265–272, <https://doi.org/10.12693/APhysPolA.140.265>.
- [26] A. Jajarmi, D. Baleanu, K. Zarghami Vahid, H. Mohammadi Pirouz, J.H. Asad, A new and general fractional Lagrangian approach: A capacitor microphone case study, *Results Phys.* 31 (2021) 104950, <https://doi.org/10.1016/j.rinp.2021.104950>.
- [27] D. Baleanu, F.A. Ghassabzade, J.J. Nieto, A. Jajarmi, On a new and generalized fractional model for a real cholera outbreak, *Alexandria Eng. J.* 61 (2022) 9175–9186, <https://doi.org/10.1016/j.aej.2022.02.054>.
- [28] M.M. S. P, MRI brain tumour segmentation using hybrid clustering and classification by back propagation algorithm, *Asian Pac. J. Cancer Prev.* 19 (2018) 3257–3263. <https://doi.org/10.31557/APJCP.2018.19.11.3257>.
- [29] S. Iqbal, J. Sheetlani, Application of Modified K means clustering algorithm in segmentation of medical images of brain tumor, *Biosci., Biotechnol. Res. Asia.* 14 (2017) 735–739, <https://doi.org/10.13005/bbra/2502>.

Further reading

- [11] C. Cattani, H.M. Srivastava, X.J. Yang, (Eds.) *Fractional dynamics*. Walter de Gruyter GmbH & Co KG. 2015.